Nucleotide Binding and Nucleotide Hydrolysis Properties of the ABC Transporter MRP6 (*ABCC6*)†

Jie Cai,‡ Roni Daoud,§ Omar Alqawi,§ Elias Georges,§ Jerry Pelletier,‡,|| and Philippe Gros*,‡,||

Department of Biochemistry, McGill Cancer Center, and Institute of Parasitology, McGill University, Montreal, Quebec, Canada H3G 1Y6

Received November 21, 2001; Revised Manuscript Received March 5, 2002

ABSTRACT: Mutations in the *MRP* gene family member *MRP6* cause pseudoxanthoma elasticum (PXE) in humans, a disease affecting elasticity of connective tissues. The normal function of MRP6, including its physiological substrate(s), remains unknown. To address these issues, recombinant rat Mrp6 (rMrp6) was expressed in the methylotrophic yeast *Pichia pastoris*. The protein was expressed in the membrane fraction as a stable 170 kDa protein. Its nucleotide binding and hydrolysis properties were investigated using the photoactive ATP analogue 8-azido-[α-^{32}P]ATP and compared to those of the drug efflux pump MRP1. rMrp6 can bind 8-azido-[α-^{32}P]ATP in a Mg^{2+}-dependent and EDTA-sensitive fashion. Co^{2+}, Mn^{2+}, and Ni^{2+} can also support 8-azido-[α-^{32}P]ATP binding by rMrp6 while Ca^{2+}, Cd^{2+}, and Zn^{2+} cannot. Under hydrolysis conditions (at 37 °C), the phosphate analogue beryllium fluoride (BeF_x) can stimulate trapping of the 8-azido-[α-^{32}P]adenosine nucleotide in rMrp6 (and in MRP1) in a divalent cation-dependent and temperature-sensitive fashion. This suggests active ATPase activity, followed by trapping and photocross-linking of the 8-azido-[α-^{32}P]ADP to the protein. By contrast to MRP1, orthovanadate-stimulated nucleotide trapping in rMrp6 does not occur in the presence of Mg^{2+} but can be detected with Ni^{2+} ions, suggesting structural and/or functional differences between the two proteins. The rMrp6 protein can be specifically photolabeled by a fluorescent photoactive drug analogue, [^{125}I]-IAARh123, with characteristics similar to those previously reported for MRP1 (*1*), and this photolabeling of rMrp6 can be modulated by several structurally unrelated compounds. The *P. pastoris* expression system has allowed demonstration of ATP binding and ATP hydrolysis by rMrp6. In addition to providing large amounts of active protein for detailed biochemical studies, this system should also prove useful to identify potential rMrp6 substrates in [^{125}I]-IAARh123 photolabeling competition studies, as well as to study the molecular basis of PXE mutations, which are most often found in the NBD2 of MRP6.

The ABC[1] transporter MRP1 (multidrug resistance associated protein 1) was discovered by its ability to cause multidrug resistance when overexpressed in tumor cells (*2*). Within the ABC transporter family, MRP1 defines a subgroup characterized by a unique N-terminal membrane associated domain composed of 5 TM segments, in addition to the 12 TM domains, and a two nucleotide binding domain (NBD) structure characteristic of many ABC transporters (*3*, *4*). Transport studies in MRP1-positive cells and membrane vesicles derived from them have demonstrated that MRP1 is a drug efflux pump that transports drugs conjugated to glutathione (GSH), glucuronide, or sulfate or even unmodified drugs together with GSH (*2*, *5*−*7*). The substrate specificity of MRP1 is broad and includes etoposide, steroid glucuronides, cysteinyl leukotrienes, dinitrophenylglutathione, and bile salt derivatives (*6*−*11*). Drug transport by MRP1 is strictly ATP-dependent (*2*), and MRP1 can be photolabeled by 8-azido-[α-^{32}P]ATP in the presence of Mg^{2+} and the transition state analogue vanadate (*1*, *12*). Vanadate-induced nucleotide trapping in MRP1 is stimulated by anticancer drugs and glutathione (*1*, *12*), and MRP1 purified and reconstituted in liposomes shows vanadate-sensitive ATPase activity that can be stimulated by several transport substrates (*13*, *14*).

MRP1 defines a gene family of at least seven, and possibly eight, members in humans (*MRP1*−*8*) (*15*−*17*) that share between ∼30% and ∼60% amino acid sequence identity. The MRP family can de divided into two subgroups based on the presence (in MRP1, -2, -3, -6, and -7) or absence (in

† This work was supported by research grants to P.G. from the National Cancer Institute of Canada and to E.G. and J.P. from the Canadian Institute for Health Research (CIHR). P.G. is an International Research Scholar of the Howard Hughes Medical Institute and is a Distinguished Scientist of the Canadian Institutes of Health Research.

* To whom correspondence should be addressed at the Department of Biochemistry, McGill University, 3655 Sir William Osler Promenade, Room 907, Montreal, Quebec, Canada H3G-1Y6. Phone: 514-398-7291. Fax: 514-398-2603. E-mail: gros@med.mcgill.ca.

‡ Department of Biochemistry, McGill University.

§ Institute of Parasitology, McGill University.

|| McGill Cancer Center, McGill University.

[1] Abbreviations: ABC, ATP binding cassette; BeF_x, beryllium fluoride; BSA, bovine serum albumin; EDTA, ethylenediaminetetraacetic acid; EGTA, ethylene glycol bis(β-aminoethyl ether)-*N*,*N*,*N*′,*N*′-tetraacetic acid; GS-X, glutathione conjugates; HA, hemagglutinin A; IAARh123, iodoarylazido-Rhodamine 123; kDa, kilodalton; MRP/Mrp, multidrug resistance associated protein; NBD, nucleotide binding domain; P-gp, P-glycoprotein; P_i, phosphate; PXE, pseudoxathoma elasticum; RT-PCR, reverse transcriptase−polymerase chain reaction; SDS−PAGE, sodium dodecyl sulfate−polyacrylamide gel electrophoresis; TM, transmembrane; UV, ultraviolet; V_i (or VO_4^{3-}), orthovanadate.

10.1021/bi012082p CCC: $22.00
Published on Web 05/30/2002

MRP4 and -5) of the 5 TM segment containing amino-terminal domain (*15*, *16*). Several MRP family members function as GS-X pumps that play key physiological roles, and mutations in these genes cause important pathologies. MRP2 (cMOAT) is expressed in the canalicular domain of hepatocytes where it transports a wide range of anionic conjugates into the biliary space (*18*−*20*), and mutations in *MRP2* cause Dubin−Johnson syndrome in humans (*18*, *21*). Increased MRP2 protein expression in transfected cells is associated with increased resistance to natural product drugs and to cisplatinum (*22*, *23*). MRP3 transports glucuronide conjugates and methotrexate (*24*), and MRP3 overexpression in transfected cells causes a low level of resistance to VP16 and teniposide (*25*). Studies on mRNA expression in lung carcinoma cell lines and in primary lung tumors indicate a correlation between increased *MRP3* mRNA expression and exposure to or resistance to cisplatinum or carboplatinum (*26*, *27*). Recent studies on MRP4 and MRP5 showed that both proteins are able to transport cyclic nucleotides cGMP and cAMP (*28*−*30*). Overexpression of MRP4 or MRP5 causes increased cellular resistance to the antiviral nucleoside analogue 9-(2-phosphonylmethoxyethyl)adenine (PMEA) and to anticancer thiopurines, 6-mercaptopurine (6-MP) and thioguanine (*28*, *30*, *31*). MRP4 can also cause resistance to short-term exposure to methotrexate but not to natural product anticancer drugs (*32*). The recently discovered MRP7 and MRP8 proteins remain uncharacterized, with respect to either their natural substrates or normal physiological function including a possible role in drug resistance (*16*, *17*).

A poorly characterized but clinically relevant MRP family member is MRP6. Initially cloned as a full-length cDNA from rat liver mRNA, rat *mrp6* mRNA (also called *mlp1* for MRP-like protein) was found to be abundantly expressed in kidney and liver of both Sprague-Dawley (SD) and Eisai hyperbilirubinemic (EHBR) rats (*33*, *34*). The human *MRP6* gene maps immediately adjacent and within 9 kb of *MRP1* on human chromosome 16p13 (*35*). The human *MRP6* encodes a protein of 1503 amino acid residues which shares 45% identity and 55% similarity with *MRP1*, its most closely related *MRP* homologue, suggesting that both genes may have emerged from a recent gene duplication event. Expression of *MRP6* mRNA was found to be increased in certain drug-resistant cell lines but was always concomitant to increased expression and amplification of the neighboring *MRP1* gene (*35*). Interestingly, an anthracycline resistance gene, *ARA*, was found to contain the 3′ half of human *MRP6* fused at the 5′ end to a short segment of *MRP1* and was shown to be amplified and overexpressed in a drug-resistant leukemic cell line (*35*, *36*). Despite close sequence identity with MRP1, the rat Mrp6 (rMrp6) protein does not appear capable of conferring drug resistance in transfected mammalian cells (Cai and Gros, unpublished). The biochemical and physiological function of MRP6 protein remains unknown. Studies in membrane vesicles from rMrp6-expressing Sf9 cells indicate that, unlike MRP1 and MRP2, rMrp6 does not transport phase II biotransformation products such as glucuronide, sulfate, or glutathione conjugates (*34*). So far, the only identified transport substrate for rMrp6 is the cyclic pentapeptide endothelin-1 receptor antagonist BQ123 (K_m ~17 μM), although endothelin-1 itself is not a substrate (*34*). In rat liver, rMrp6 protein is expressed mostly in the lateral membrane of hepatocytes with weaker staining at the canalicular membrane (*33*, *34*). This location is also difficult to reconcile with a role for rMrp6 in biliary secretion.

Recently, human *MRP6* (*ABCC6*) was found mutated in patients with pseudoxanthoma elasticum (PXE) (*37*−*40*). PXE is a inherited disorder of connective tissues, characterized by calcification of elastic fibers in skin, arteries, and retina that results in dermal lesions with associated loss of elasticity, arterial insufficiency, and retinal bleeding leading to macular degeneration (*41*). PXE presents both recessive and dominant modes of inheritance, and the *MRP6* gene initially mapped to chromosome 16p13.1 (*42*, *43*) was isolated by positional cloning. Mutational analysis of *MRP6* in PXE patients identified a variety of genetic lesions, including large and small deletions, splicing mutations, nonsense mutations, and a number of mis-sense mutations (*37*−*40*). Interestingly, most of the single amino acid substitutions mapped in NBD2 of MRP6 (R1114P, R1138Q/W, R1314W, W1259G, R1268Q) with none in NBD1. They are presumed to behave as loss of function, highlighting the key role of NBD2 site in MRP6 protein activity. Subsequent expression studies of *MRP6* mRNA by RT-PCR in tissues affected in PXE patients have revealed low *MRP6* expression in skin, retina, vessel walls, and placenta (*38*). However, the substrate specificity, mechanism of transport, and role of MRP6 in PXE remain completely unknown.

To begin addressing these questions, we have overexpressed the rat Mrp6 protein in the methylotrophic yeast *Pichia pastoris*. The protein is stable and abundant in membrane fractions from rMrp6-expressing *P. pastoris* cells, and photolabeling studies with 8-azido-[α-^{32}P]ATP under binding or trapping conditions indicate that the protein can bind and hydrolyze ATP. Comparative studies with MRP1 using different transition state analogues identify important differences between the two proteins. Thus, this *P. pastoris* expression system can be used to characterize the biochemical properties of MRP6/Mrp6 and can be used to study the molecular basis of loss-of-function mutations found in PXE patients.

MATERIALS AND METHODS

Materials. Oligonucleotides used to clone rat *mrp*6 (*mlp*1) recombinant cDNA fragments and to assemble a full-length clone were obtained from Gibco BRL (Montreal, Quebec, Canada). Mouse monoclonal anti-hemagglutinin (HA) antibody 16B12 was purchased from Babco Laboratories (Richmond, CA). The *P. pastoris* expression system, including the expression plasmid vector pHIL-D2 and the tester strains GS115 and KM71, was purchased from Invitrogen (license no. 145457). 8-Azido-[α-^{32}P]ATP (specific activity of 8−15 Ci/mmol) was purchased from Affinity Labeling Technologies Inc. (Lexington, KY). [^{125}I]-IAARh123 was chemically synthesized and labeled as previously described (*44*). Taq DNA polymerase was from Gibco BRL (Montreal, Quebec, Canada), and all restriction enzymes were from New England Biolabs (Mississauga, Ontario, Canada). All other chemicals were of the highest commercial grade available.

Cloning of Rat mrp6 (mlp1) cDNA. Three juxtaposed cDNA fragments, with approximate sizes of 2.2, 1.35, and 1.0 kb, respectively, were generated by RT-PCR using poly-

$(A)^+$ RNA from rat liver. For RNA isolation, freshly dissected liver was homogenized in 8 M guanidinium isothiocyanate by mechanical disruption, and total RNA was isolated by further centrifugation through a CsCl cushion according to Sambrook and Russell (*45*). The polyadenylated fraction of this RNA was isolated by two successive steps of affinity chromatography on oligo(dT)−cellulose using standard protocols (*45*), with the final product recovered by ethanol precipitation. For RT-PCR, oligo(dT) was used to prime first-strand cDNA synthesis (*46*), and rat *mrp6* was further amplified from the cDNA pool using three pairs of sequence-specific oligonucleotides derived from public sequences (GenBank Accession Number AB010466) (*33*). The three pairs of *mrp*6-specific primers were JC300 (5′-CATGAATTCACCATGAACGGAGAGCACTCA-3′) and JC302 (5′-GGCACAGGCTTCTAGAACTTC-3′), JC301 (5′-GAAGTTCTAGAAGCCTGTGCC-3′) and JC304 (5′-CCCCAGGAGCTCCAGGTTG-3′), and JC303 (5′-GCCAACCTGGAGCTCCTGG-3′) and JC305 (5′-GTTGAGCTCGAATTCTGGGAAGAGTCCTGACTCAG-3′). The three resulting cDNA fragments were cloned into pBluescript/KS^+ and assembled into a full-length *mrp*6 cDNA to generate plasmid pBS4.5.100. Sequence analysis of this clone identified a double nucleotide change (G389C and C390G) from that of the published sequence, which results in a Ser to Thr substitution (at amino acid residue 122) within the first membrane-associated domain of the protein. The nature of this sequence variation remains unclear at the present. Nonetheless, this single amino acid substitution is unlikely to affect the function of the protein, since it occurs within a protein segment, the sequence of which is not conserved in other MRP family members. To clone *mrp*6 cDNA into the methylotrophic yeast *P. pastoris* expression vector pHIL-D2, a *Sac*II site followed by a favorable translation initiation context sequence was introduced immediately upstream of the first ATG initiation codon (underlined) by PCR-mediated mutagenesis using oligos JC322 (5′-ATCCCGCGGAACCATGAACGGAGAGCACTC-3′) and JC308 (5′-CTCCTGGCGGAAGCTCC-3′). Also, the 3′ end of the *mrp6* cDNA was modified by elimination of the natural termination codon and insertion of a supplementary sequence containing an HA epitope (YPYDVPDYAS) (*3*). This sequence was introduced into *mrp6* cDNA using a combination of PCR mutagenesis and double-stranded oligonucleotide insertion as we have previously described (*1*). The 4.5 kb *mrp6* cDNA tagged at the C-terminus with an HA epitope tag was recovered using inserted *Sac*II and *Sna*BI sites, followed by cloning into the *Sac*II/*Sna*BI sites of a modified pHIL-D2 vector (*1*), which results in a recombinant protein also containing six consecutive histidine residues immediately following the HA epitope at its extreme C-terminus. The resulting plasmid was termed pHIL-*mrp*6-cHA-His_6. The integrity of all *mrp*6-containing plasmids was confirmed by restriction analysis and by DNA sequencing.

Generation of rMrp6 Expressing Clones in P. pastoris. Transformation of pHIL-*mrp*6-cHA-His_6 and pHIL-D2 into *P. pastoris* GS115 (*his4*, Mut^+) and KM71 (*arg4*, *his4*, *aox1::ARG4*, Mut^s) strains was carried out using a lithium chloride method, exactly as previously described (*1*). Clones overexpressing the recombinant rMrp6-cHA-His_6 protein (presented as rMrp6 throughout the rest of the paper) in either strain were identified by Western blotting analysis of crude membrane preparations from randomly picked His^+ (KM71) or His^+/Mut^s transformants (GS115) after methanol induction, using the mouse anti-HA monoclonal antibody. The vector plasmid pHIL-D2 was also transformed in both *P. pastoris* strains under the same conditions, and individual clones were randomly picked as negative controls.

Plasma Membrane Preparation and Immunoblotting Analyses. Small- and large-scale membrane fractions were prepared from *P. pastoris* using a combination of lysis by French pressure cell and multistep ultracentrifugation, as previously described (*1*). The protein content of such fractions was determined by the Bradford protein assay (Bio-Rad) using BSA as a standard. To identify *P. pastoris* clones that overexpress rMrp6 recombinant protein, crude membrane proteins (5 μg) from *mrp6*- and vector-transformed *P. pastoris* cells were resolved on SDS−PAGE (7.5%) and transferred on nitrocellulose membranes. Western blotting analyses were performed using mouse anti-HA monoclonal antibody 16B12, and horseradish peroxidase- (HRP-) conjugated sheep anti-mouse (for anti-HA) IgG as the secondary antibody.

Photolabeling of rMrp6 Protein with 8-Azido-[α-^{32}P]ATP. The photolabeling studies with 8-azido-[α-^{32}P]ATP were carried out essentially as previously described (*1*) with slight modifications. Briefly, crude membranes (20 μg) were incubated with 5 μM 8-azido-[α-^{32}P]-ATP in the presence of 3 mM $MgCl_2$ in TEG buffer containing 40 mM Tris-HCl, pH 7.4, and 0.1 mM EGTA (total reaction volume was 20 μL) for 10 min, either on ice (for nucleotide binding analysis) or at 37 °C (for nucleotide trapping analysis). Transition analogues such as beryllium fluoride (BeF_x at 5 mM) or orthovanadate (VO_4^{3-} at 0.2 mM) were included in nucleotide trapping analysis as indicated in the figures. In certain experiments, variations on these conditions were introduced and are described in the legends of the individual figures. To test the effects of different nucleotides on nucleotide trapping by rMrp6, membrane proteins were preincubated with unlabeled nucleotides for 5 min at room temperature (23 °C) before addition of radiolabeled nucleotide. Reactions were started by addition of radiolabeled nucleotide. After incubation for the indicated times, the unbound components were removed by centrifugation (245000*g*, 30 min, 4 °C). The protein pellets were washed once with 100 μL of ice-cold TEG buffer, resuspended in 12 μL of ice-cold TEG buffer, and subjected to UV irradiation (5 min on ice; λ = 260 nm; UVS-II Minerallight, model R52, UVP Inc., San Gabriel, CA). The protein samples were dissolved in Laemmli sample buffer and separated by SDS−PAGE (7.5%). Gels were stained with Coomassie brilliant blue R250 and dried, followed by autoradiography by exposure to Kodak X-AR films with an intensifying screen at −80 °C.

Photoaffinity Labeling with [^{125}I]-IAARh123. Photoaffinity labeling of rMrp6 with [^{125}I]-IAARh123, binding competition assay, and immunoprecipitation of photolabeled rMrp6 protein using anti-HA monoclonal antibody were carried out as described (*1*). Samples were resolved by Fairbank's gel electrophoresis. The gels were dried and exposed to Kodak X-AR films at −80 °C. Quantitative analysis was performed using the PhosphorImaging Scanning system and the ImageQuaNT program as described (*1*).

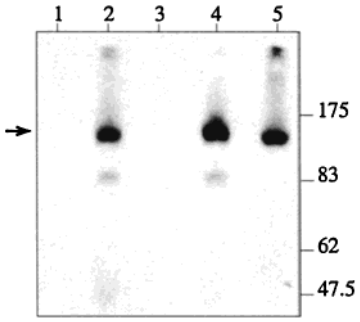

FIGURE 1: Immunodetection of rMrp6 expression in *P. pastoris* using anti-HA monoclonal antibody. Five micrograms of total membrane proteins was dissolved in sample buffer, separated by SDS−PAGE (7.5%), and analyzed by immunoblotting as described in Materials and Methods. Lanes 1 and 3 are crude membrane proteins from plasmid vector pHIL-D2 transformed GS115 and KM71 strain (negative controls), respectively. Lanes 2 and 4 are from GS115/*mrp6*-cHA-His_6 and KM71/*mrp6*-cHA-His_6 transformants, respectively. Lane 5 is from a KM71/*MRP1*-cHA-His_6 transformant (*1*), used as a positive control. The position of molecular mass markers (in kDa) is shown on the right side of the figure. The arrow indicates the position of the full-length, immunoreactive rMrp6-cHA-His_6 recombinant protein.

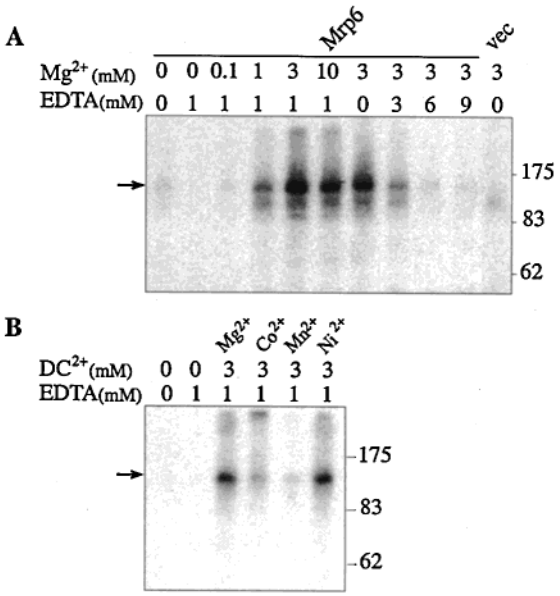

FIGURE 2: Requirement for divalent cations for nucleotide binding by rMrp6. Crude membrane proteins (20 μg) from KM71/*mrp6*-cHA-His_6 transformants (Mrp6) or from KM71 plasmid vector pHIL-D2 transformants (vec) were incubated with 8-N_3-[α-^{32}P]ATP in labeling buffer under nucleotide binding conditions (4 °C, 10 min) in the presence of varying concentrations of Mg^{2+} and EDTA (A) or various divalent cations (DC^{2+}) (B), as indicated. Excess nucleotide was removed by centrifugation, followed by UV cross-linking, and labeled products (in total membrane proteins) were analyzed by SDS−PAGE and autoradiography (Materials and Methods). Photolabeled rMrp6 protein is identified by arrows, and molecular mass standards (in kDa) are indicated on the right side of the figure.

RESULTS

Expression of rMrp6 in the Yeast P. pastoris. At the time of inception of these experiments, only the rat *mrp*6 cDNA was publicly available, and RT-PCR was used to reclone a full-length copy of the rat *mrp6* cDNA (see Materials and Methods). We have previously used the methylotrophic yeast *P. pastoris* for high-level expression and ultimately for purification of the ABC transporters P-glycoprotein (Pgp) (*47*) and MRP1 (*1*). Both Pgp and MRP1 expressed in *Pichia* remain fully active and display robust substrate-stimulated ATPase activity. Therefore, the rat *mrp6* cDNA was modified by in-frame addition at the C-terminus of an HA epitope tag and a hexahistidine segment, followed by cloning into the *P. pastoris* expression vector pHIL-D2 (pHIL-*mrp*6-cHA-His_6). These modifications were introduced to facilitate detection of the recombinant protein and future purification studies. The recombinant plasmid pHIL-*mrp*6-cHA-His_6 was introduced into *P. pastoris* strains GS115 and KM71, and rMrp6 expressing clones were identified by Western blotting using the 16B12 anti-HA monoclonal antibody as described in Materials and Methods (Figure 1). About 5−10% of the His^+ *mrp6* transformants were detected positive for rMrp6 expression by anti-HA antibody. Expression of the recombinant rMrp6 protein in these clones was verified using a specific rabbit anti-rMrp6 polyclonal antiserum (data not shown). As shown in Figure 1, rMrp6 is readily detectable in the membrane fraction of both GS115 and KM71 transformants. The protein appears stable and migrates with an apparent molecular mass of 160−170 kDa, in good agreement with the size predicted from the primary amino acid sequence (165 kDa). The majority of the rMrp6 recombinant protein expressed in *P. pastoris* was detected as a full-length protein, although a small amount of a 75−85 kDa immunoreative band was specifically detected in *Pichia/mrp6* transformants (Figure 1). This may represent a minor proteolytic product of the full-length protein present in the crude membrane extract.

8-Azido[α*-*^{32}*P]ATP Binding to rMrp6 Expressed in P. pastoris.* rMrp6 is a member of the ABC superfamily of membrane transporters (*33*). As such, rMrp6 shows two predicted nucleotide binding sites (NBS), and BQ123 transport by rMrp6 in membrane vesicles is ATP-dependent (*34*). Therefore, it is reasonable to presume that functional rMrp6 should be capable of binding and hydrolyzing ATP. To test the ATP binding properties of rMrp6, a labeling assay using the hydrolyzable, photoactive ATP analogue 8-azido-[α-^{32}P]ATP was implemented (*1*). Briefly, crude membrane fractions from control *P. pastoris* cells or from rMrp6-expressing cells were incubated on ice with 8-azido-[α-^{32}P]-ATP (binding conditions). Unbound ligand was removed by ultracentrifugation, and membranes were resuspended prior to UV cross-linking and analysis of the photolabeled products by SDS−PAGE (Figure 2A). In these experiments, the requirement of Mg^{2+} ions for 8-azido-[α-^{32}P]ATP binding was further investigated by varying the concentrations of Mg^{2+} and EDTA in the labeling reaction. In the absence of Mg^{2+} in the labeling reaction (either with or without EDTA), no significant labeling was detected in the membrane of rMrp6-expressing cells. Upon increasing Mg^{2+} concentration (in the presence of EDTA fixed at 1 mM), a protein species of apparent molecular mass 160−170 kDa could be readily labeled by 8-azido-[α-^{32}P]ATP (Figure 2A). Labeling appeared specific and was limited to a single major species, which was absent from membrane fractions of cells transformed with the plasmid vector (vec). The apparent molecular mass of the photolabeled protein was similar to that detected by immunoblotting with the anti-HA antiobody in the same membrane fractions (Figure 1). A Mg^{2+} concentration of approximately 3 mM seemed optimal for photolabeling, which was well maintained up to 10 mM Mg^{2+}, and

increasing the molar excess of EDTA progressively abolished photolabeling of rMrp6 (Figure 2A). These results show that rMrp6 expressed in *P. pastoris* membranes is properly folded and can bind 8-azido-[α-^{32}P]ATP. In addition, 8-azido-[α-^{32}P]ATP binding by rMrp6 is strictly dependent on the presence of Mg^{2+} ions. The requirement of specific divalent cations for 8-azido-[α-^{32}P]ATP binding by rMrp6 was further investigated using a number of divalent cations substituted for Mg^{2+} in the labeling reaction. It was observed that Co^{2+}, Mn^{2+}, and Ni^{2+} could also support 8-azido-[α-^{32}P]ATP binding by rMrp6 (Figure 2B), whereas photolabeling in the presence of Ca^{2+}, Cd^{2+}, and Zn^{2+} did not yield photolabeled rMrp6 (data not shown).

Nucleotide Trapping by rMrp6 Is Stimulated by Beryllium Fluoride. In the case of ABC transporters such as MRP1, ATP hydrolysis leads to the formation of a high-energy protein·Mg·ADP*P_i intermediate, which is proposed to cause a major structural change in the protein during transport. Phosphate analogues such as orthovanadate (V_i) can replace P_i in the catalytic site, leading to the formation of stably inhibited enzyme complexed to these analogues. In the case of MRP1 (*1*, *12*) and P-gp (*48*), the protein·MgADP·V_i inhibited state can be visualized by photo-cross-linking the azido group of 8-azido-[α-^{32}P]ATP to the protein under nucleotide hydrolysis conditions (37 °C). Indeed, vanadate-induced trapping of nucleotides has been used extensively as an indicator of MRP1 and P-gp ATPase activity in protein preparations from mammalian and yeast cells (*1*, *12*, *49*−*51*). To test possible ATPase activity of rMrp6, crude membrane fractions from rMrp6-expressing *P. pastoris* cells were incubated with 8-azido-[α-^{32}P]ATP for 10 min at 37 °C (hydrolysis conditions), in the presence or absence of V_i. Trapped complexes were recovered by centrifugation, cross-linked with UV, and analyzed by SDS−PAGE and autoradiography (Figure 3A). In membrane fractions from control MRP1-expressing *P. pastoris* cells, there was little, if any, specific labeling of the protein by 8-azido-[α-^{32}P]ATP in the absence of V_i. However, addition of 0.2 mM V_i caused dramatic nucleotide trapping in MRP1, leading to the appearance of a strongly labeled 165 kDa protein which was absent from control vector transformed cells (vec) (Figure 3A). Very different results were obtained with rMrp6-positive membranes. First, and as opposed to MRP1, rMrp6 could be labeled by 8-azido-[α-^{32}P]ATP under hydrolysis conditions in the absence of V_i. This labeling was specific (absent from control membranes, vec in Figure 3A), required the presence of Mg^{2+} ions, and probably represented 8-azido-[α-^{32}P]ATP binding to the protein, in agreement with results from Figure 2A. Second, labeling of rMrp6 under these conditions was not stimulated by V_i at the range of concentrations tested (between 0.02 and 1 mM) (Figure 3A). This behavior is unique and clearly different from that of MRP1 and P-gp where photolabeling under hydrolysis conditions is strictly V_i-dependent (*1*, *52*).

The observed lack of V_i-stimulated nucleotide trapping in rMrp6 can be interpreted alternatively as an intrinsic lack of ATPase activity of the protein or may be an artifactual loss of function of an otherwise active ATPase possibly associated with expression in *P. pastoris*. Alternatively, rMrp6 expressed in *P. pastoris* may be active, but V_i may not be a suitable transition state analogue for efficient trapping of the hydrolyzed nucleotide (8-azido-[α-^{32}P]ADP)

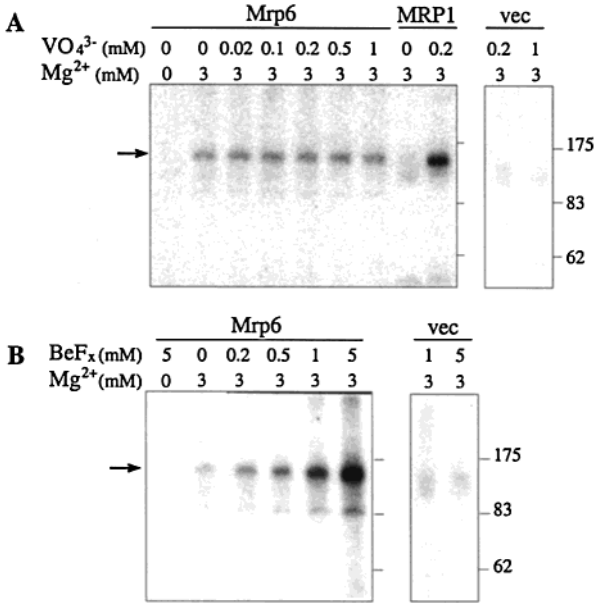

FIGURE 3: Trapping of nucleotides in rMrp6 in the presence of increasing concentrations of orthovanadate (VO_4^{3-}; A) or beryllium fluoride (BeF_x; B). Nucleotide trapping was carried out under nucleotide hydrolysis conditions. Crude membrane proteins (20 μg) from KM71/*mrp6*-cHA-His_6 transformants (Mrp6), KM71/*MRP1*-cHA-His_6 transformants [MRP1 (*1*)], or KM71 plasmid vector pHIL-D2 transformants (vec) were incubated with 8-N_3-[α-^{32}P]ATP (37 °C, 10 min), followed by cross-linking and SDS−PAGE as described in the legend to Figure 2 and in Materials and Methods. Photolabeled rMrp6 protein is identified by arrows, and molecular mass standards (in kDa) are indicated on the right side of the figure.

in the NB site(s) of rMrp6. Beryllium fluoride is a transition state analogue and potent inhibitor of several ATPases, including F_1-ATPase (*53*, *54*), myosin (*55*), and P-gp (*56*, *57*). Recently, it was shown that BeF_x can induce trapping of 8-azido-[α-^{32}P]ADP in P-gp (*56*, *57*). BeF_x is structurally distinct from V_i, and the Mg·ADP·BeF_x·protein complex has the conformation of the prehydrolysis, MgATP-bound complex (*58*). Therefore, we tested whether BeF_x could induce trapping of 8-azido-[α-^{32}P]ATP in rMrp6. For this, control and rMrp6-positive membranes were incubated with 8-azido-[α-^{32}P]ATP and increasing concentrations of BeF_x (in the form of beryllium sulfate and sodium fluoride mix at 1:5 molar ratio) under hydrolysis conditions (10 min, 37 °C), and the resulting cross-linked photolabeled complexes were analyzed by SDS−PAGE (Figure 3B). Under these conditions, photolabeling of rMrp6 by 8-azido-[α-^{32}P]ATP was readily stimulated by BeF_x. Stimulation of photolabeling was found to be concentration-dependent and was optimal at 5 mM of BeF_x (Figure 3B). BeF_x stimulation of rMrp6 photolabeling by 8-azido-[α-^{32}P]ATP could reflect either increased stability of the Mg·8-azido-[α-^{32}P]ATP·protein complex or effective BeF_x-mediated trapping of the hydrolyzed Mg·8-azido-[α-^{32}P]ADP·BeF_x·protein complex. To distinguish between the two, the temperature dependence of BeF_x-stimulated photolabeling was analyzed. Results in Figure 4A clearly show that the BeF_x-induced trapping of nucleotide was temperature-dependent, reached maximal at 37 °C, and was absent at 4 °C. By contrast, V_i used in the same conditions showed no stimulation of rMrp6 photolabeling either at 37 or at 4 °C (Figure 4B). These results suggest that the observed BeF_x stimulation of rMrp6 labeling reflects hydrolysis and subsequent trapping of the Mg·8-

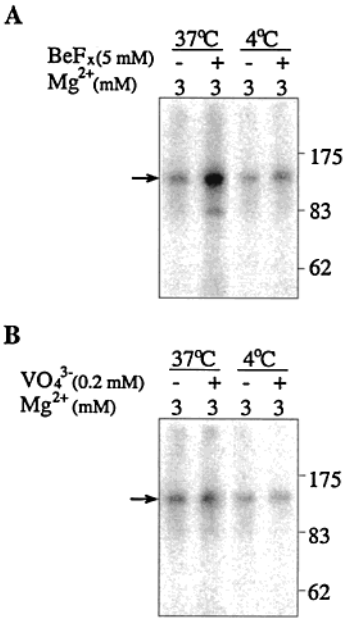

FIGURE 4: Temperature dependence of nucleotide trapping by rMrp6. Crude membrane proteins (20 μg) from KM71/*mrp6*-cHA-His_6 transformants (Mrp6) were incubated with 8-N_3-[α-^{32}P]ATP in labeling buffer in the absence or presence of either beryllium fluoride (BeF_x; A) or orthovanadate (VO_4^{3-}; B), at either 37 or 4 °C for 10 min. UV-mediated cross-linking, SDS−PAGE, and radioautography were as described in the legend to Figure 2 and in Materials and Methods. Photolabeled rMrp6 protein is identified by arrows, and molecular mass standards (in kDa) are indicated on the right side of the figure.

azido-[α-^{32}P]ADP·BeF_x·protein complex, implying that rMrp6 expressed in *P. pastoris* is catalytically active and capable of ATP hydrolysis.

Beryllium Fluoride Stimulated Trapping of Nucleotide in rMrp6 Is Dependent on Divalent Cations. The requirement for divalent cations in the noted BeF_x-induced trapping of nucleotide in rMrp6 was investigated by carrying out the photolabeling reaction in the presence of 5 mM BeF_x and of various concentrations of Mg^{2+} and EDTA (Figure 5A). Results from these experiments showed that BeF_x stimulation of nucleotide trapping by rMrp6 (hydrolysis conditions) is strictly dependent on the presence of Mg^{2+} ions, with an optimal concentration estimated at between 3 and 10 mM. Depletion of Mg^{2+} by addition of EDTA completely inhibited photolabeling of rMrp6. The divalent cation selectivity of the BeF_x-stimulated nucleotide trapping in rMrp6 was investigated (Figure 5B). In those experiments, MRP1-positive membranes were analyzed in identical conditions and used as controls for comparative analysis. For rMrp6, the low level of trapping seen in control conditions (−BeF_x) was strongly stimulated by BeF_x in a divalent cation dependent manner. Mg^{2+}, Co^{2+}, and Mn^{2+}, as well as Ni^{2+}, can all support this effect (Figure 5B, left panel). Interestingly, nucleotide trapping in MRP1 could also be stimulated by BeF_x (Figure 5B, right panel). In control conditions (−BeF_x), no trapping could be detected, but BeF_x could readily induce trapping in MRP1, and all divalent cations tested could support this stimulation. Moreover, V_i, which was used as an additional control in these experiments, stimulated nucleotide trapping into MRP1 in the presence of all four divalent cations (Figure 5C, right panel) but failed to do so in rMrp6 in the presence of Mg^{2+}, Co^{2+}, and Mn^{2+},

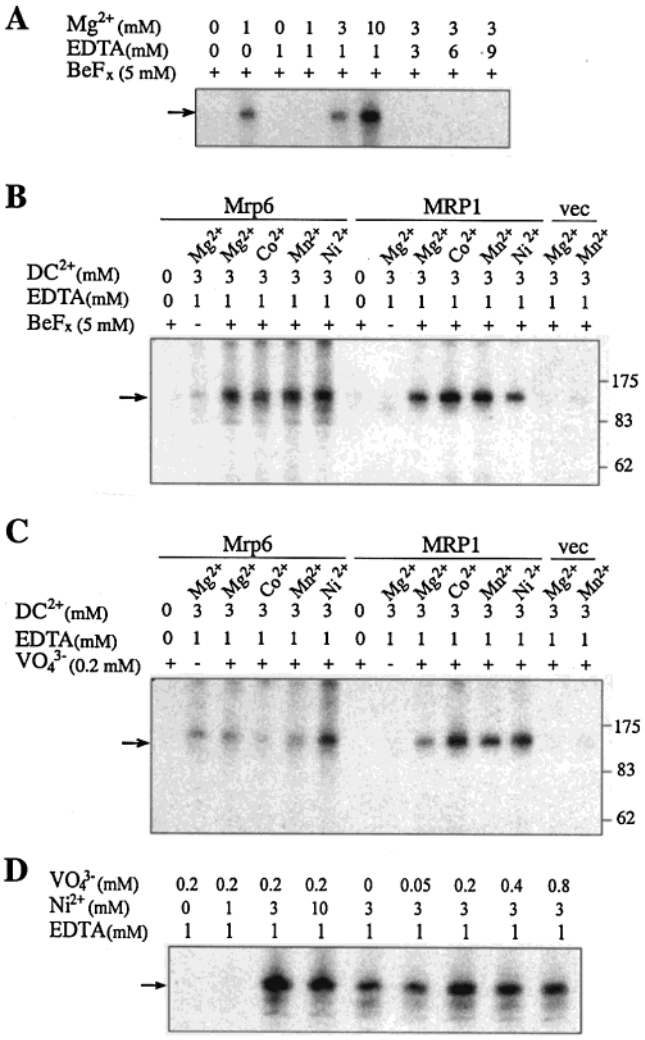

FIGURE 5: Divalent cation dependence of orthovanadate and beryllium fluoride induced nucleotide trapping in rMrp6. Crude membrane proteins (20 μg) from KM71/*mrp6*-cHA-His_6 transformants (rMrp6), KM71/*MRP1*-cHA-His_6 transformants (MRP1; *1*), or KM71 plasmid vector pHIL-D2 transformants (vec) were incubated with 8-N_3-[α-^{32}P]ATP under hydrolysis conditions (37 °C, 10 min) in various divalent cations. (A) Magnesium (Mg^{2+}) dependence of BeF_x-induced nucleotide trapping in rMrp6 was analyzed in buffers containing different concentrations of Mg^{2+} ions and in the absence or presence of EDTA (indicated). The selectivity for Mg^{2+}, Co^{2+}, Mn^{2+}, and Ni^{2+} of orthovanadate (VO_4^{3-}; B) or beryllium fluoride (BeF_x; C) induced trapping of nucleotide in either rMrp6 or MRP1 was also tested. (D) V_i-induced nucleotide trapping in rMrp6 mediated by nickel (Ni^{2+}). UV-mediated cross-linking, SDS−PAGE, and radioautography were as described in the legend to Figure 2 and in Materials and Methods. Photolabeled rMrp6 protein is identified by arrows, and molecular mass standards (in kDa) are indicated on the right side of the figure.

except for Ni^{2+} (Figure 5C, left panel). As shown in Figure 5D, Ni^{2+} can mediate V_i-stimulated nucleotide trapping at a range of concentrations similar to that of Mg^{2+} in BeF_x-stimulated nucleotide trapping (Figure 5A). In addition, the concentration of V_i required to achieve an optimal level of nucleotide trapping in the presence of Ni^{2+} is 0.2 mM, identical to that required for V_i-induced nucleotide trapping in MRP1 (*1*).

To delineate the nucleotide substrate specificity for rMrp6, BeF_x-induced trapping of 8-azido-[α-^{32}P] nucleotide in rMrp6 was carried out in the presence of increasing concentrations (0−250 μM) of various nucleotides. ATP (Figure 6A) and,

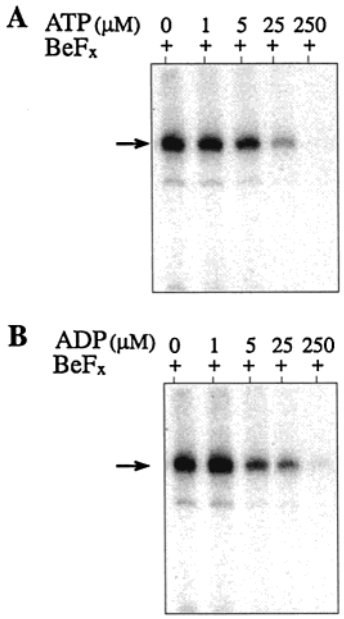

FIGURE 6: Competition of beryllium fluoride induced nucleotide trapping in rMrp6 by unlabeled di- or trinucleotides. Crude membrane proteins (20 μg) from KM71/*mrp6*-cHA-His_6 transformants (Mrp6) were preincubated with increasing concentrations of ATP (A) or ADP (B) for 5 min at 20 °C, prior to the addition of 8-N_3-[α-^{32}P]ATP, Mg^{2+} (3 mM), and beryllium fluoride (BeF_x at 5 mM), followed by incubation under hydrolysis conditions (37 °C, 10 min). UV-mediated cross-linking, SDS−PAGE, and radioautography were as described in the legend to Figure 2 and in Materials and Methods. Photolabeled rMrp6 protein is identified by arrows.

to a lesser extent, CTP (data not shown) showed a concentration-dependent competition of BeF_x-induced nucleotide trapping, whereas GTP and UTP were not effective competitors (data not shown). Interestingly, ADP also acted as an efficient inhibitor of nucleotide trapping by rMrp6 (Figure 6B), in agreement with the proposal that the trapped nucleotide is in the form of ADP, in the inhibited Mg^{2+}·nucleotide·BeF_x· protein complex.

Photolabeling of rMrp6 with [^{125}I]Iodoarylazido-Rhodamine 123. We have previously shown that MRP1 expressed in *P. pastoris* can be photolabeled by a radiolabeled photoactivatable analogue of Rhodamine, [^{125}I]-IAARh123. Photolabeling of MRP1 by [^{125}I]-IAARh123 can be competed by different MRP1 substrates (*1*, *44*), and binding of the probe involves two protein segments located near TM10 and TM11 and near TM16 and TM17 (*59*). To test whether rMrp6 could also bind [^{125}I]-IAARh123, membrane from control and rMrp6-expressing cells was incubated with [^{125}I]-IAARh123, followed by UV cross-linking, analysis by Fairbank's gel electrophoresis, and autoradiography (Figure 7A). [^{125}I]-IAARh123 labeled a number of proteins in membrane fractions from both control and rMrp6-expressing cells; however, a specific polypeptide of 160−170 kDa was uniquely labeled in rMrp6 membranes (Figure 7A, left panel). Immunoprecipitation of the labeled membranes with a mouse monoclonal anti-HA antibody confirmed that this [^{125}I]-IAARh123 reactive protein was indeed rMrp6 (Figure 7A, right panel). Binding of the probe to rMrp6 was found to be concentration-dependent and saturated at approximately 4 μM (Figure 7B). To further characterize this photoaffinity labeling of rMrp6, a competition assay was carried out (Figure 8) as previously described (*1*). It was found that

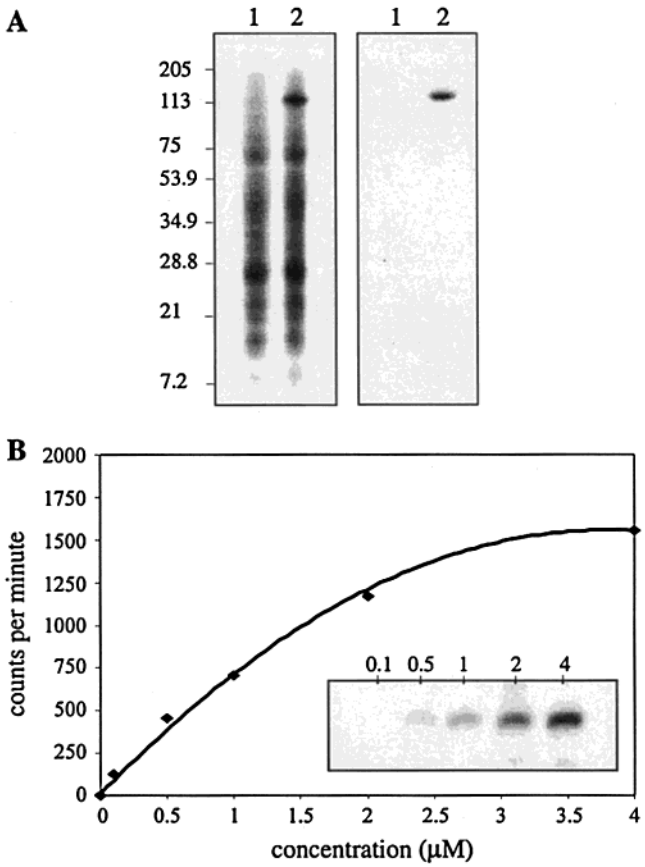

FIGURE 7: Photoaffinity labeling of Mrp6 by [^{125}I]-IAARh123. (A) Autoradiogram of the photoaffinity labeling reaction of membrane proteins (20 μg) from control KM71/pHIL-D2 (lane 1) and KM71/m*rp6*-cHA-His_6 (lane 2) cells with 1 μM [^{125}I]-IAARh123 as described in Materials and Methods. The reaction mixtures were analyzed either directly by Fairbank's gel electrophoresis (left panel) or after immunoprecipitation of rMrp6 with anti-HA monoclonal antibody (right panel). The molecular mass standards (in kDa) are shown on the left side of the figure. (B) Quantification of the labeled rMrp6 band was carried out using ImageQuaNT, and the results were plotted against the concentrations of ligand that were used in the labeling reaction.

photoaffinity labeling of rMrp6 was inhibited by the MDR drugs VBL and DOX, as well as by the LTD_4 receptor antagonist MK571, yet unaffected by the MRP1 substrates LTC_4 and VP-16. More interestingly, the photolabeling of rMrp6 appeared stimulated by BQ123, the endothelin-1 receptor antagonist known to be transported by this protein (*34*). Together, these results indicate that rMrp6 can bind [^{125}I]-IAARh123 with characteristics similar to that previously reported for MRP1 (*1*). However, the effect of other compounds on this binding is not identical to that observed for MRP1, suggesting differences in substrate specificity between the two proteins.

DISCUSSION

MRP1 and MRP6 are two ABC transporters and the most closely related members of the MRP family. The chromosomal proximity of the *MRP1* and *MRP6* genes on human chromosome 16 (*35*) is unique in the *MRP* gene family and suggests that the two genes arose from recent in situ duplication of a common ancestor, followed by evolutionary drift and sequence divergence. The implications of such sequence divergence on common or specific structural and

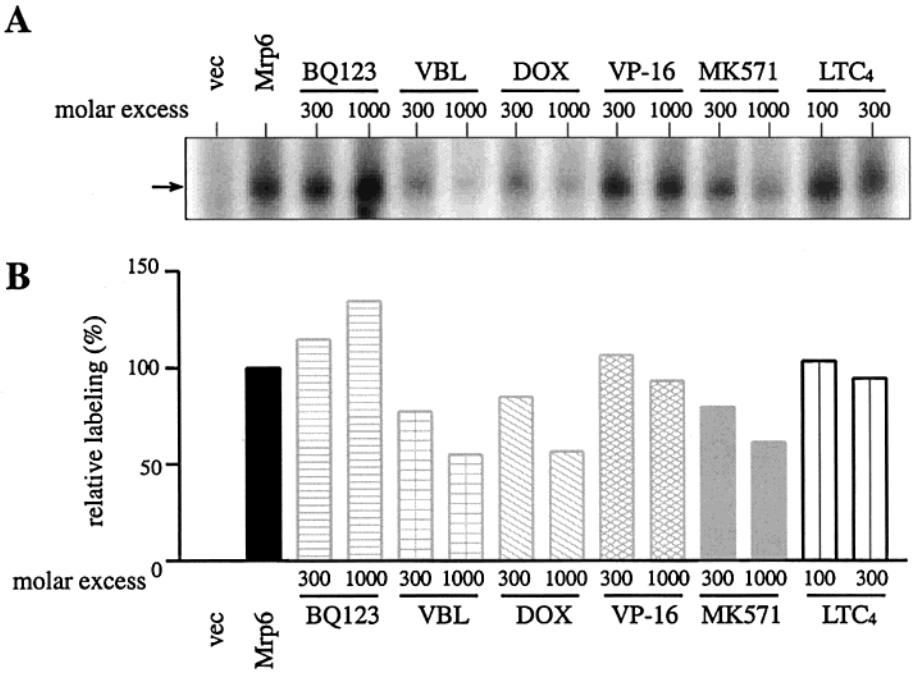

FIGURE 8: Competition of photoaffinity labeling of rMrp6 by [^{125}I]-IAARh123. The photoaffinity labeling reactions were carried out in the absence or presence of a molar excess of various compounds as indicated. Lane 1 (left) is the negative control reaction with crude membrane proteins from control KM71/pHIL-D2 cells. All of the other lanes are reactions with crude membrane proteins from KM71/*Mrp6*-cHA-His$_6$ cells. (A) Autoradiogram of the photoaffinity label products. The photolabeled rMrp6 protein is indicated by an arrow. (B) Quantification of the photoaffinity labeling of rMrp6 by [^{125}I]-IAARh123 using ImageQuaNT. The relative labeling of rMrp6 in the absence of competitors (positive control in lane 2) is set as 100%. The effect of competing ligands on rMrp6 labeling is presented as a percentage of the amount of remaining photolabeling in rMrp6 in each reaction relative to that in the positive control sample (lane 2).

functional aspects of each protein remain poorly characterized. MRP1 and rMrp6 proteins share 58% sequence identity in NBD1, 62% in NBD2, and between 35% and 45% in the membrane-associated portions of the proteins (*33*). Despite this close similarity, significant functional differences have been noted: As opposed to MRP1, rMrp6 does not confer drug resistance (Cai and Gros, unpublished) and does not transport chemotherapeutic drugs or phase 2 biotransformation products (*34*). Since membrane-associated domains of MRP1 have been previously shown to mediate drug binding (*44*, *60*), the low-level sequence similarity in these regions of MRP1 and rMrp6 may indeed underline different substrate specificity for these two proteins. Nevertheless, MRP6 plays an important physiological role, and mutations in this gene cause PXE in humans (*37*−*39*). PXE is a disease of connective tissue characterized by premature degradation of elastin fibers, with pleiotropic consequences for ocular, vascular, and other structures. Therefore, characterizing the mechanism of action of MRP6 including identifying its normal physiological substrate is important to understand the role of MRP6 in the physiopathology of PXE. Mutational analysis in PXE patients provides some interesting clues, as it shows that most mutations map in or near NBD2. As PXE mutations are presumed to represent loss of function, this suggests that (a) NBD2 is essential for MRP6 function, (b) it may be more mutation-sensitive than NBD1, and (c) it may be possibly reflecting structural and/or functional differences between the two NB sites of MRP6.

To begin addressing these issues, we have expressed rMrp6 in the yeast *P. pastoris* and have characterized the nucleotide binding and hydrolysis properties of the protein. We have previously shown that P-gp and MRP1 expressed in *P. pastoris* are fully functional, can bind and hydrolyze ATP, bind drug analogues, and show substrate-stimulated vanadate-induced trapping of nucleotides (*1*, *47*, *61*). Further, a large amount of active P-gp has been purified from *P. pastoris* for structural studies, by use of a simple affinity chromatography protocol (*62*). Here, we show that rMrp6 can be stably expressed at high levels in the membrane fraction of *P. pastoris*. The nucleotide binding and hydrolysis properties of rMrp6 were studied and compared to those of MRP1, revealing some similarities and some notable differences. Under relatively "stringent" nucleotide binding conditions consisting of incubation of membranes with 8-azido-[α-^{32}P]-ATP (5 μM) at 4 °C, followed by removal of unbound ligands by centrifugation prior to cross-linking with UV, rMrp6 can be readily photolabeled (Figure 2). By contrast, MRP1 showed very little labeling in these conditions and requires a substantially higher concentration of 8-azido-[α-^{32}P]ATP (*1*). Labeling of rMrp6 under these conditions is specific, temperature-independent, and EDTA-sensitive and most likely corresponds to nucleotide binding to the protein. Increased labeling of rMrp6 compared to MRP1 may reflect higher affinity of rMrp6 for 8-azido-[α-^{32}P]ATP. The two proteins also showed different properties with respect to interaction with transition state analogues. Molecules such as V_i, BeF_x, and AlF_4 are structurally related to, and can substitute for, P_i in the nucleotide binding site, leading to a stably inhibited enzyme with the hydrolyzed nucleotide trapped in the site. When 8-azido-[α-^{32}P]ATP is used as a substrate, labeled azido-ADP can be cross-linked in the site by UV irradiation, thereby providing a convenient way to assess ATP hydrolysis in the protein. We have previously reported substrate-stimulated, vanadate-induced trapping of P-gp (*63*) and MRP1 (*1*) expressed in *Pichia*. In this study, we could demonstrate BeF_x-stimulated trapping of nucleotide

in both MRP1 and rMrp6 (Figure 3). BeF_x stimulation required Mg^{2+} ions and occurred only at 37 °C, consistent with ATPase activity by both proteins with concomitant trapping of ADP in one or both NB sites. Interestingly, the BeF_x stimulation of nucleotide trapping in MRP1 and rMrp6 displayed somewhat different selectivity for divalent cations. Importantly and by contrast to MRP1, no stimulatory effect of orthovanadate on 8-azido-[α-^{32}P]ATP labeling of rMrp6 could be observed in the presence of Mg^{2+}. However, when Ni^{2+} was used in replacement of Mg^{2+}, an induction of nucleotide trapping by orthovanadate was observed in rMrp6 (Figure 5D), suggesting that vanadate-induced nucleotide trapping can occur in rMrp6 under certain circumstances. The relevance of this finding is unknown, as Ni^{2+} is unlikely to be naturally available to support ATP binding in rMrp6. Together, these studies show that, like MRP1, rMrp6 can indeed bind and hydrolyze ATP.

Results from both divalent cation selectivity and transition state analogue studies all suggest important structural and possibly functional differences between the NB sites of the two proteins with respect to interaction with Mg·ADP/ATP. The three-dimensional structure of the MgADP·V_i (*64*), MgADP·AlF_4, and MgADP·BeF_x (*58*) complexes in the nucleotide binding site has been determined for myosin. The V_i and AlF_4 inhibited complexes are very similar and display a bond length of 2.0 Å between the V/Al atoms and the pseudobridging oxygen (O) of the β-phosphorus of ADP. This bond length is significantly longer than the 1.56 and 1.67 Å bond length for the O atoms between the β- and α-phosphate groups of ADP, an observation strongly supporting the proposal that MgADP·V_i and MgADP·AlF_4 complexes are true analogues of the P_i*ADP transition state. On the other hand, the bond length measured for the Be to β-O bond in the MgADP·BeF_x inhibited complex is 1.57 Å and very similar to that seen for the P−O bond linking the α- and β-phosphates. This indicates that the MgADP·BeF_x complex looks exactly like ATP bound in the active site, reflecting the "ground" state of the enzyme prior to hydrolysis (*58*, *64*). Therefore, our findings suggest that although MRP1 and rMrp6 can produce stable MgADP·BeF_x complexes, the V_i inhibited complex cannot be stabilized in rMrp6 in the presence of Mg^{2+} and, thus, is not detected by cross-linking. In the case of myosin, stabilization of the MgADP·BeF_x and MgADP·V_i complexes in the binding pocket requires additional H−protein bonds originating from sets of residues and water molecules that are different in both structures. Therefore, different availability of such amide protons in MRP1 and rMrp6 may contribute to different stability of the BeF_x and V_i complexes in each protein. Taken together, these results suggest that although both proteins can bind and hydrolyze ATP, structural differences may exist between the NB sites of both proteins.

The normal physiological function of MRP6 remains unknown, including the nature of the transported substrates, which may be impaired in PXE patients. Transfection and overexpression of rMrp6 in either CHO cells or LLCPK cells do not confer drug resistance to hydrophobic natural product chemotherapeutic drugs (Cai and Gros, unpublished). Likewise, transport studies in membrane vesicles failed to detect rMrp6 transport activity for either hydrophobic MDR drugs, various glutathione, glucuronide, and sulfate conjugates, prostaglandins, and various aminophospholipids (*34*). Similarly, we could not detect stimulation of BeF_x-induced trapping of azidoadenosine nucleotide in rMrp6 by any of these groups of substrates (data not shown). So far, the only known transport substrate for rMrp6 is the anionic cyclic pentapeptide BQ-123 (*34*). BQ-123 is a structural analogue of endothelin-1, behaving as an endothelin-1 receptor antagonist, a finding of potential interest since vasculature is one of the tissues affected in PXE patients. However, it was observed that endothelin-1 itself was not transported by rMrp6, although it was a substrate for the MRP2/cMOAT homologue (*34*). Nonetheless, no significant effect of BQ-123 on 8-azidoadenosine nucleotide trapping by rMrp6 was observed (data not shown). In the present study, we observe that the photoactivatable Rhodamine 123 (Rh123) derivative iodoarylazido-Rh123 (IAARh123) can interact specifically with rMrp6 in cross-linking experiments, with apparent affinity in the low micromolar range (Figure 7). This property may prove useful in the identification and validation of possible natural rMrp6 transport substrates and possibly in acting as competitive inhibitors of photolabeling by IAARh123. To this end, competition studies were carried out, in which rMRP6 was preincubated with different hydrophobic compounds prior to photolabeling by [^{125}I]-IAARh123. Photolabeling of rMrp6 could be inhibited by VBL, DOX, and MK571 but was not affected by LTC_4 and VP-16, the two preferred substrates of MRP1. Surprisingly, the only known substrate of rMRP6 BQ123 appeared to stimulate photolabeling of the protein at high concentrations (at 1000-fold molar excess). These results suggest that rMrp6 can seemingly interact with a number of structurally unrelated molecules. However, these competition experiments also suggest that rMrp6 and MRP1 may have different substrate specificity.

Finally, the stable expression of rMrp6 in a functional state in *P. pastoris* may allow the isolation of purified rMrp6 in large amounts, a necessary prerequisite to detailed functional characterization and for ultimate structural studies of the protein, such as infrared or fluorescence spectroscopy.

REFERENCES

1. Cai, J., Daoud, R., Georges, E., and Gros, P. (2001) *Biochemistry 40*, 8307−8316.
2. Hipfner, D. R., Mao, Q., Qiu, W., Leslie, E. M., Gao, M., Deeley, R. G., and Cole, S. P. (1999) *J. Biol. Chem. 274*, 15420−15426.
3. Kast, C., and Gros, P. (1997) *J. Biol. Chem. 272*, 26479−26487.
4. Kast, C., and Gros, P. (1998) *Biochemistry 37*, 2305−2313.
5. Keppler, D., Leier, I., and Jedlitschky, G. (1997) *Biol. Chem. 378*, 787−791.
6. Loe, D. W., Almquist, K. C., Cole, S. P., and Deeley, R. G. (1996) *J. Biol. Chem. 271*, 9683−9689.
7. Loe, D. W., Almquist, K. C., Deeley, R. G., and Cole, S. P. (1996) *J. Biol. Chem. 271*, 9675−9682.
8. Loe, D. W., Deeley, R. G., and Cole, S. P. (1996) *Eur. J. Cancer 32A*, 945−957.
9. Leier, I., Jedlitschky, G., Buchholz, U., Cole, S. P., Deeley, R. G., and Keppler, D. (1994) *J. Biol. Chem. 269*, 27807−27810.
10. Muller, M., Meijer, C., Zaman, G. J., Borst, P., Scheper, R. J., Mulder, N. H., de Vries, E. G., and Jansen, P. L. (1994) *Proc. Natl. Acad. Sci. U.S.A. 91*, 13033−13037.
11. Zaman, G. J., Versantvoort, C. H., Smit, J. J., Eijdems, E. W., de Haas, M., Smith, A. J., Broxterman, H. J., Mulder, N. H., de Vries, E. G., Baas, F., et al. (1993) *Cancer Res. 53*, 1747−1750.
12. Taguchi, Y., Yoshida, A., Takada, Y., Komano, T., and Ueda, K. (1997) *FEBS Lett. 401*, 11−14.
13. Chang, X. B., Hou, Y. X., and Riordan, J. R. (1997) *J. Biol. Chem. 272*, 30962−30968.

14. Mao, Q., Leslie, E. M., Deeley, R. G., and Cole, S. P. (1999) *Biochim. Biophys. Acta 1461*, 69−82.
15. Borst, P., Evers, R., Kool, M., and Wijnholds, J. (2000) *J. Natl. Cancer Inst. 92*, 1295−1302.
16. Hopper, E., Belinsky, M. G., Zeng, H., Tosolini, A., Testa, J. R., and Kruh, G. D. (2001) *Cancer Let.t 162*, 181−191.
17. Bera, T. K., Lee, S., Salvatore, G., Lee, B., and Pastan, I. H. (2001) *Mol. Med. 7*, 509−516.
18. Paulusma, C. C., Kool, M., Bosma, P. J., Scheffer, G. L., ter Borg, F., Scheper, R. J., Tytgat, G. N., Borst, P., Baas, F., and Oude Elferink, R. P. (1997) *Hepatology 25*, 1539−1542.
19. Paulusma, C. C., and Oude Elferink, R. P. (1997) *J. Mol. Med. 75*, 420−428.
20. Ito, K., Fujimori, M., Nakata, S., Hama, Y., Shingu, K., Kobayashi, S., Tsuchiya, S., Kohno, K., Kuwano, M., and Amano, J. (1998) *Oncol. Res. 10*, 99−109.
21. Kartenbeck, J., Leuschner, U., Mayer, R., and Keppler, D. (1996) *Hepatology 23*, 1061−1066.
22. Evers, R., Kool, M., van Deemter, L., Janssen, H., Calafat, J., Oomen, L. C., Paulusma, C. C., Oude Elferink, R. P., Baas, F., Schinkel, A. H., and Borst, P. (1998) *J. Clin. Invest. 101*, 1310−1319.
23. Cui, Y., Konig, J., Buchholz, J. K., Spring, H., Leier, I., and Keppler, D. (1999) *Mol. Pharmacol. 55*, 929−937.
24. Hirohashi, T., Suzuki, H., and Sugiyama, Y. (1999) *J. Biol. Chem. 274*, 15181−15185.
25. Kool, M., van der Linden, M., de Haas, M., Scheffer, G. L., de Vree, J. M., Smith, A. J., Jansen, G., Peters, G. J., Ponne, N., Scheper, R. J., Elferink, R. P., Baas, F., and Borst, P. (1999) *Proc. Natl. Acad. Sci. U.S.A. 96*, 6914−6919.
26. Yang, X., Uziely, B., Groshen, S., Lukas, J., Israel, V., Russell, C., Dunnington, G., Formenti, S., Muggia, F., and Press, M. F. (1999) *Lab. Invest. 79*, 271−280.
27. Oguri, T., Isobe, T., Fujitaka, K., Ishikawa, N., and Kohno, N. (2001) *Int. J. Cancer 93*, 584−589.
28. Jedlitschky, G., Burchell, B., and Keppler, D. (2000) *J. Biol. Chem. 275*, 30069−30074.
29. Wijnholds, J., Mol, C. A., van Deemter, L., de Haas, M., Scheffer, G. L., Baas, F., Beijnen, J. H., Scheper, R. J., Hatse, S., De Clercq, E., Balzarini, J., and Borst, P. (2000) *Proc. Natl. Acad. Sci. U.S.A. 97*, 7476−7481.
30. Chen, Z. S., Lee, K., and Kruh, G. D. (2001) *J. Biol. Chem. 276*, 33747−33754.
31. Schuetz, J. D., Connelly, M. C., Sun, D., Paibir, S. G., Flynn, P. M., Srinivas, R. V., Kumar, A., and Fridland, A. (1999) *Nat. Med. 5*, 1048−1051.
32. Lee, K., Klein-Szanto, A. J., and Kruh, G. D. (2000) *J. Natl. Cancer Inst. 92*, 1934−1940.
33. Hirohashi, T., Suzuki, H., Ito, K., Ogawa, K., Kume, K., Shimizu, T., and Sugiyama, Y. (1998) *Mol. Pharmacol. 53*, 1068−1075.
34. Madon, J., Hagenbuch, B., Landmann, L., Meier, P. J., and Stieger, B. (2000) *Mol. Pharmacol. 57*, 634−641.
35. Kool, M., van der Linden, M., de Haas, M., Baas, F., and Borst, P. (1999) *Cancer Res. 59*, 175−182.
36. Davey, R. A., Longhurst, T. J., Davey, M. W., Belov, L., Harvie, R. M., Hancox, D., and Wheeler, H. (1995) *Leukocyte Res. 19*, 275−282.
37. Le Saux, O., Urban, Z., Tschuch, C., Csiszar, K., Bacchelli, B., Quaglino, D., Pasquali-Ronchetti, I., Pope, F. M., Richards, A., Terry, S., Bercovitch, L., de Paepe, A., and Boyd, C. D. (2000) *Nat. Genet. 25*, 223−227.
38. Bergen, A. A., Plomp, A. S., Schuurman, E. J., Terry, S., Breuning, M., Dauwerse, H., Swart, J., Kool, M., van Soest, S., Baas, F., ten Brink, J. B., and de Jong, P. T. (2000) *Nat. Genet. 25*, 228−231.
39. Ringpfeil, F., Lebwohl, M. G., and Uitto, J. (2000) *J. Invest. Dermatol. 115*, 332.
40. Ringpfeil, F., Pulkkinen, L., and Uitto, J. (2001) *Exp. Dermatol. 10*, 221−228.
41. Uitto, J., Pulkkinen, L., and Ringpfeil, F. (2001) *Trends Mol. Med. 7*, 13−17.
42. Struk, B., Neldner, K. H., Rao, V. S., St Jean, P., and Lindpaintner, K. (1997) *Hum. Mol. Genet. 6*, 1823−1828.
43. Cai, L., Struk, B., Adams, M. D., Ji, W., Haaf, T., Kang, H. L., Dho, S. H., Xu, X., Ringpfeil, F., Nancarrow, J., Zach, S., Schaen, L., Stumm, M., Niu, T., Chung, J., Lunze, K., Verrecchia, B., Goldsmith, L. A., Viljoen, D., Figuera, L. E., Fuchs, W., Lebwohl, M., Uitto, J., Richards, R., Hohl, D., and Ramesar, R. (2000) *J. Mol. Med. 78*, 36−46.
44. Daoud, R., Kast, C., Gros, P., and Georges, E. (2000) *Biochemistry 39*, 15344−15352.
45. Sambrook, J., and Russell, D. W. (2001) *Molecular Cloning: A Laboratory Manual*, 3rd ed., Cold Spring Harbor Press, Cold Spring Harbor, NY.
46. Epstein, D. J., Vekemans, M., and Gros, P. (1991) *Cell 67*, 767−774.
47. Beaudet, L., Urbatsch, I. L., and Gros, P. (1998) *Methods Enzymol. 292*, 397−413.
48. Urbatsch, I. L., Sankaran, B., Bhagat, S., and Senior, A. E. (1995) *J. Biol. Chem. 270*, 26956−26961.
49. Gao, M., Cui, H. R., Loe, D. W., Grant, C. E., Almquist, K. C., Cole, S. P., and Deeley, R. G. (2000) *J. Biol. Chem. 275*, 13098−13108.
50. Hou, Y., Cui, L., Riordan, J. R., and Chang, X. (2000) *J. Biol. Chem. 275*, 20280−20287.
51. Nagata, K., Nishitani, M., Matsuo, M., Kioka, N., Amachi, T., and Ueda, K. (2000) *J. Biol. Chem. 275*, 17626−17630.
52. Urbatsch, I. L., Sankaran, B., Weber, J., and Senior, A. E. (1995) *J. Biol. Chem. 270*, 19383−19390.
53. Issartel, J. P., Dupuis, A., Lunardi, J., and Vignais, P. V. (1991) *Biochemistry 30*, 4726−4733.
54. Issartel, J. P., Dupuis, A., Morat, C., and Girardet, J. L. (1991) *Eur. Biophys. J. 20*, 115−126.
55. Phan, B. C., Faller, L. D., and Reisler, E. (1993) *Biochemistry 32*, 7712−7719.
56. Sankaran, B., Bhagat, S., and Senior, A. E. (1997) *Biochemistry 36*, 6847−6853.
57. Sankaran, B., Bhagat, S., and Senior, A. E. (1997) *Arch. Biochem. Biophys. 341*, 160−169.
58. Fisher, A. J., Smith, C. A., Thoden, J. B., Smith, R., Sutoh, K., Holden, H. M., and Rayment, I. (1995) *Biochemistry 34*, 8960−8972.
59. Daoud, R., Julien, M., Gros, P., and Georges, E. (2001) *J. Biol. Chem. 276*, 12324−12330.
60. Daoud, R., Desneves, J., Deady, L. W., Tilley, L., Scheper, R. J., Gros, P., and Georges, E. (2000) *Biochemistry 39*, 6094−6102.
61. Urbatsch, I. L., Beaudet, L., Carrier, I., and Gros, P. (1998) *Biochemistry 37*, 4592−4602.
62. Julien, M., Kajiji, S., Kaback, R. H., and Gros, P. (2000) *Biochemistry 39*, 75−85.
63. Urbatsch, I. L., Julien, M., Carrier, I., Rousseau, M. E., Cayrol, R., and Gros, P. (2000) *Biochemistry 39*, 14138−14149.
64. Smith, C. A., and Rayment, I. (1996) *Biochemistry 35*, 5404−5417.

BI012082P